Hindawi
Advances in Materials Science and Engineering
Volume 2018, Article ID 5728174, 16 pages
https://doi.org/10.1155/2018/5728174

Research Article

Effect of Mean Stress on the Fatigue Life Prediction of Notched Fiber-Reinforced 2060 Al-Li Alloy Laminates under Spectrum Loading

Weiying Meng[1,2], **Liyang Xie**[1,2], **Yu Zhang**[3], **Yawen Wang**[4], **Xiaofang Sun**[5] and **Shijian Zhang**[1,2]

[1]*Institute of Modern Design and Analysis, College of Mechanical Engineering & Automation, Northeastern University, Shenyang 110819, China*
[2]*Key Laboratory of Vibration and Control of Aero-Propulsion Systems Ministry of Education of China, Northeastern University, Shenyang 110819, China*
[3]*School of Mechanical Engineering, Shenyang Jianzhu University, Shenyang 110168, China*
[4]*Department of Mechanical and Aerospace Engineering, University of Texas at Arlington, Arlington, TX 76019, USA*
[5]*College of Science, Shenyang Jianzhu University, Shenyang 110168, China*

Correspondence should be addressed to Weiying Meng; mengweiying025@163.com

Received 24 December 2017; Revised 17 March 2018; Accepted 22 March 2018; Published 6 June 2018

Academic Editor: Frederic Dumur

This paper presents a study on the fatigue life prediction of notched fiber-reinforced 2060 Al-Li alloy laminates under spectrum loading by applying the constant life diagram. Firstly, a review on the state of the art of constant life diagram models for the life prediction of composite materials is given, which highlights the effect on the forecast accuracy. Then, the fatigue life of notched fiber-reinforced Al-Li alloy laminates (2/1 laminates and 3/2 laminates) is tested under cyclic stress, which has different stress cycle characteristics (constant amplitude loading and Mini-Twist spectrum loading). The introduced models are successfully realized based on the available experimental data of examined laminates. In the case of Mini-Twist spectrum loading, the effect of the constant life diagram on the life prediction accuracy of examined laminates is studied based on the rainflow-counting method and Miner damage criteria. The results show that the simple Goodman model and piecewise linear model have certain advantages compared to other complex models for the life prediction of notched fiber metal laminates with different structures under Mini-Twist loading. From the engineering perspective, the S-N curve prediction based on the piecewise linear model is most applicable and accurate among all the models.

1. Introduction

Fiber metal laminates (Arall and Glare et al.), as the new generation of aircraft structural materials, are the best alternatives for aluminum materials [1]. These laminates are composed of the metal layers and the fiber-reinforced resin layer, and these fibers can be placed in different directions [2]. Compared with conventional materials (metals or fiber-reinforced epoxy resin composites), fiber metal laminates could enhance the mechanical property by combining the metal layer and fiber layer, which exhibit excellent fatigue and impact properties and allow for flexible structural designs. Currently, fiber metal laminates have been used in the fuselage, leading edge, and other parts of the Airbus [3–6]. In view of the abovementioned advantages, fiber metal laminates have the potential wide application in aerospace equipment. Thus, understanding their fatigue performance is very important.

In general, fatigue strength is often referring to the structural strength under constant amplitude fatigue loading. However, constant amplitude loading is too ideal for engineering structures in practice. Therefore, variable amplitude cyclic stress should be considered [7]. In addition, not only the smooth material is used in actual engineering,

but also notched materials are used more frequently. Since the failure mechanism of the smooth material is different from that of the notched material, the study on the fatigue properties of the notched material is also necessary. In the past few decades, the fatigue life prediction of composites under variable amplitude cyclic stress has received increasing interests. At the same time, the fatigue properties of the notched composite material are also widely concerned.

The life prediction problem of unnotched composite materials under variable amplitude loading is mainly based on the theory of fatigue damage cumulative and progressive fatigue damage. Some researchers have made some achievements in the application of fatigue damage cumulative theory to predict the fatigue life. A fatigue damage cumulative model for the fiber-reinforced plastics (FRPs) under variable amplitude loading was presented by Yao and Himmel [8], which was assumed that the damage state of laminates could be described phenomenologically by residual strength. A review on damage accumulation rules and residual strength approaches for FRP materials subjected to spectrum loading was made by Post [9], and the prediction accuracy of these introduced models was compared and analyzed. The effects of the cycle-counting method, constant life diagram formulation, and damage accumulation theory on the life prediction problem for composite materials under spectrum loading were discussed by Passipoularidis and Philippidis [10]. The fatigue properties of carbon fiber-reinforced plastic laminates under variable amplitude loading were studied by Hosoi et al. [7], who found that damage cumulative under variable amplitude loading could be better described by considering residual strength. Some researchers have also made some progress in the study of progressive fatigue damage theory for life prediction. In order to simulate the damage process of composite laminates under fatigue loading, a progressive fatigue damage model was first proposed by Shokrieh and Lessard [11]. Based on the fatigue test of the unidirectional laminates, the fatigue life prediction system of composite laminates was constructed by the three-part cyclical process of stress analysis, failure analysis, and material performance degradation. A progressive damage model applied in fatigue life prediction for composites under block and spectrum loading was discussed by Passipoularidis et al. [12], who used classical lamination theory to perform stress analysis, applied the failure criterion of Puck to implement adequate stiffness discount tactics, and merged residual strength into fatigue damage accumulation criteria. Fatigue properties of notched composites under variable amplitude loading have also been studied by some scholars. In order to increase the life prediction accuracy of notched composite materials under spectrum loading, an improved progressive damage model was proposed by Hu et al. [13]. In the model, a stiffness-strength degradation coupled model which was related to the damage of composites was developed, and a damage equivalent was made by the continuity of stiffness degradation so that it could be effectively applied to fatigue life prediction under complex loading. The fatigue crack growth model and delamination growth behavior of notched fiber metal laminates were studied by Khan et al. [14–17], who considered the effect of variable amplitude loading. A mechanism-based life prediction model of FMLs under constant amplitude loading was developed by Wu and Guo [18]. And the fatigue behaviors of GLARE laminates under single overloads were investigated experimentally and were predicted by an equivalent crack closure model. The fatigue crack growth and delamination extension behaviors of FMLs under single tensile overload were studied by Huang et al. [19], who found that fatigue crack growth and delamination behaviors could be influenced by the stress intensity factor of the crack tip in the metal layer when the overload is applied.

Studying on the potential damage mechanism of composite laminates and interpreting the relationship of feedback between materials and loading are a new research trend for the fatigue model of composite laminates [20]. The method based on the actual damage mechanism involves the properties of the fiber and matrix and the fatigue behavior of the laminate structure. However, the studies on fatigue life prediction of composites using the actual damage mechanism are restricted due to the complexity of the phenomenon [9]. As a result, the phenomenological approach has been more prevailing in the life prediction of composite materials under variable amplitude loading. It is an experienced method based on macroscopic mechanical properties of composites, which avoids the independent hypothesis units of component materials and obtains the model parameters by curve fitting. In order to verify the effectiveness of this method, composite materials with different compositions and those with different layer structures under various loading conditions have been examined by various researchers [10, 21–33].

The phenomenological approach has the same applicability for the unnotched and notched laminates, and the approach can phenomenally reflect the material damage. This is because the approach is a phenomenological empirical method that does not take into account the specific damage situation, and the model parameters can be obtained by curve fitting. The phenomenological approach for fatigue life prediction of composite materials under variable amplitude has three processes: (1) loading cycle counting, (2) the constant life diagram (CLD) model, and (3) the damage criterion. In order to determine an effective life prediction method under practical spectrum loading, some researchers have attempted to compare different models for each process [10]. Among them, the rainflow-counting method and Palmgren–Miner (PM) damage criteria are, respectively, the most widely used methods in the process of loading cycle counting and damage criterion. These CLD models are derived from different mathematical principles and based on the fatigue data of materials under constant amplitude loading. For the CLD-modeling process, it has been shown in recent studies that different models have a great impact on the fatigue life prediction accuracy of composite laminates under spectrum loading [21].

Unlike fiber-reinforced resin laminates, the fiber-reinforced metal laminates have a metallic composite

structure and a nonmetallic composite structure, which leads to a different fatigue damage mechanism. A large number of documents showed that the research of this material was mainly focused on fatigue crack propagation and delamination behavior. Generally, it is very difficult to study the fatigue life prediction under complex spectrum loading based on fatigue crack propagation and delamination behavior, and there is very few research on the fatigue life prediction for notched fiber metal laminates based on the phenomenological approach.

In this paper, different CLD models in the life prediction of composite materials are introduced and compared. The effect of CLD models on the life prediction of notched fiber-reinforced Al-Li alloy laminates under spectrum loading is the focus of this study. The applicability of the model, the requirement of the test data, and the prediction accuracy are treated as important assessment parameters. The 2/1 laminates and 3/2 laminates of the notched fiber-reinforced Al-Li alloy are tested under three kinds of cyclic stress (constant amplitude loading with the stress ratio $R = 0.06$, that with the stress ratio $R = -1$, and Mini-Twist spectrum loading). Taking the fatigue life prediction under Mini-Twist spectrum loading for two kinds of the material as an example, the effect of CLD models on life prediction under Mini-Twist spectrum loading is studied through the use of the rainflow-counting method and Miner damage criteria.

2. Life Prediction Theory for Composite Material

2.1. Composite Life Prediction. At present, the research work on fatigue life prediction of composite materials under variable amplitude mainly focuses on the phenomenological approach. For life prediction under the complex stress cycle, it is a simple and effective method. The basic mechanical properties of the examined material used as input in the calculation are the compression static strength, tension static strength, and at least one S-N curve. The implementation process of the phenomenological approach is described as follows: Firstly, the number of cycles for the applied spectrum or block loading will be counted in order to predict the fatigue life under the complex stress cycle. The rainflow method is regarded as the most common cycle-counting method used in the irregular loading spectrum and is therefore adopted in this study. Secondly, the fatigue life at desired R is evaluated by using the aforementioned material properties. An empirical model is required by most of the damage accumulation approaches to determine the total failure cycles under a constant amplitude stress which is equivalent to the current applied stress. Hence, the total failure cycles can be determined directly by the constant life diagram for a given stress cycle. The method will be later discussed in detail. Finally, the damage accumulation will be calculated. In this study, the Miner damage rule is adopted. It is a well-known and simple linear empirical rule.

2.2. Constant Life Diagram Models. Constant life diagrams are treated as a predictive tool to estimate the material fatigue life under loading patterns. It can reflect the combined effect of material properties and mean stress on the fatigue life [22]. The main parameters used to build CLD models are the cyclic stress amplitude σ_a, the mean cyclic stress σ_m, and the stress ratio R. The R is defined as the ratio of the minimum cyclic stress to the maximum cyclic stress, that is, $R = \sigma_{min}/\sigma_{max}$.

A number of CLD models have been proposed in the past to describe the characteristics of different composite materials. Based on symmetric linear Goodman and nonlinear Gerber equations, a variety of correction models are derived to simulate the behavior characteristics of composite materials [21]. The Goodman diagram is the simplest and most basic CLD and often used to verify the validity of other models. Without any assumptions, the piecewise linear (Pwlinear) interpolation was used between different S-N curves based on modified Goodman diagram concepts [23–25]. According to this idea, the analytical expressions for any desired S-N curve were proposed [26]. The piecewise nonlinear (PNL) model was developed by Anastasios, in which simple phenomenological equations were established based on the relationship between the stress amplitude σ_a and the stress ratio R [22]. In addition, the PNL model was a mathematical representation of the material's properties on the $R - \sigma_a$ plane, and the equations were derived without any assumptions. The Bell model was derived by Harris et al., and it was based on the semi-empirical formulations [27–29]. The result of this model was a continuous bell-shaped line from compressive strength to tensile strength, which was obtained from a nonlinear equation by fitting the experimental data. Based on the theory of the Gerber line, Boerstra deduced another CLD formulation [30]. In this model, the theory of variable slopes with various mean stresses for the S-N lines was introduced, and the exponent 2 of the Gerber equation was modified as a variable. This model provided a simple method for the fatigue life prediction and avoided fatigue data classification based on R values, when the laminate material was subjected to cyclic stress with continuously varying mean stress. An alleged heteromorphic CLD was derived by Kawai, and the model was established by introducing the "critical" S-N curve concept [31, 32]. The ratio of ultimate compression strength (UCS) to ultimate tensile strength (UTS) was treated as the R value of the critical S-N curve for the examined material. Based on the assumption that fatigue failure probability and static failure probability are equivalent, Kassapoglou recently developed a new CLD model [33]. Only the compressive and tensile static strength data were required to obtain the desired S-N curve in the Kassapoglou model. However, this model had an obvious drawback: it ignored different damage mechanisms resulted from fatigue stress and led to erroneous results in some cases. The models mentioned above will be described in detail below.

2.2.1. Goodman Diagram. For any cycle stress with the stress amplitude σ_a and mean stress σ_m, the equivalent stress amplitude σ_{eq} at $R = -1$ is expressed as follows:

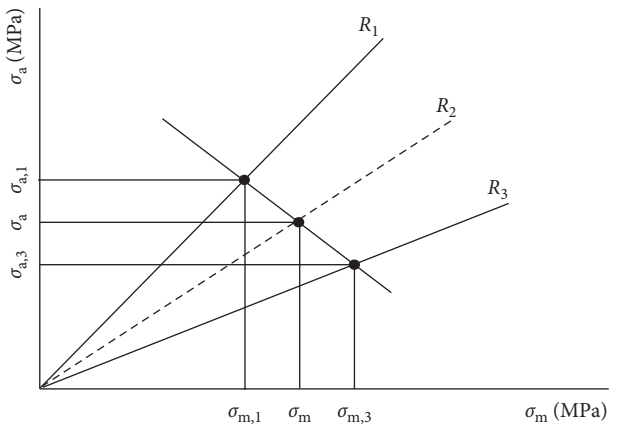

Figure 1: Illustration of the linear interpolation theory.

$$\sigma_{eq} = \frac{\sigma_a \times \mathrm{UTS}}{\mathrm{UTS} - \sigma_m} \quad \text{for } \sigma_m > 0,$$
$$\sigma_{eq} = \frac{\sigma_a \times \mathrm{UCS}}{\mathrm{UCS} - \sigma_m} \quad \text{for } \sigma_m < 0. \tag{1}$$

The equivalent stress σ_{eq} corresponding to any cycle stress can be obtained by using the above equations. It will be used as an input into the S-N curve at $R = -1$ in order to determine the allowable number of cycles N_i for the current cycle stress. The model can be used directly based on a power S-N curve or an exponential S-N curve.

2.2.2. Piecewise Linear CLD Model. The piecewise linear CLD model is deduced by linear interpolation theory between different S-N curves on the (σ_m-σ_a) plane [23–26]. This CLD model is constructed based on the compression static strength data and tension static strength data as well as a limited number of known S-N curves (generally at $R = 10$, $R = -1$, and $R = 0.1$). The S-N curves at any R values can be obtained by linear interpolation theory between experimentally determined static strength and fatigue strength data.

In this study, two experimentally determined S-N curves and static strength data are available. The unknown S-N curves can be obtained by the linear interpolation theory. The diagram of the piecewise linear model is shown in Figure 1, and the derivation process of the model is as follows. The R values of two determined S-N curves are defined as R_1 and R_3, respectively, and the R value of desired S-N curves is defined as R_2. Firstly, the mean stress $\sigma_{m,2}$ and stress ratio R_2 of the current cycle are determined. Secondly, the values of $\sigma_{m,k}$ and $\sigma_{a,k}$ ($k = 1, 3$) for known S-N curves are calculated based on the slope a_1 and intercept b_1, and the slope a_3 and intercept b_3. The position of R_1 and R_3 on the (σ_m-σ_a) plane is described by $\sigma_{m,k}$ and $\sigma_{a,k}$. The position of R_2 on the constant life plot can only be described by $\sigma_{m,2}$ and $\sigma_{a,2}$, so the exact location cannot be determined at present. Thirdly, an initial fatigue life N is assumed. When $R_k < 1.0$ ($k = 1, 3$), for the assumed life N, the corresponding formulas of mean stress and amplitude stress are shown as follows:

$$\sigma_{m,k} = \frac{(1+R_k)\sigma_{p,k}}{2} = \frac{(1+R_k)}{2} 10^{(\log(N) - b_k)/a_k}, \quad k = 1, 3,$$
$$\sigma_{a,k} = \frac{(1-R_k)\sigma_{p,k}}{2} = \frac{(1-R_k)}{2} 10^{(\log(N) - b_k)/a_k}, \quad k = 1, 3, \tag{2}$$

and when $R_k > 1.0$ ($k = 1, 3$), then

$$\sigma_{m,k} = \frac{(1+R_k)\sigma_{p,k}}{2} = -\frac{1+R_k}{2} 10^{(\log(N) - b_k)/a_k}, \quad k = 1, 3,$$
$$\sigma_{a,k} = \frac{(1-R_k)\sigma_{p,k}}{2} = -\frac{1-R_k}{2} 10^{(\log(N) - b_k)/a_k}, \quad k = 1, 3. \tag{3}$$

Fourthly, the line equation through points $\{\sigma_{m,1}, \sigma_{a,1}\}$ and $\{\sigma_{m,3}, \sigma_{a,3}\}$ on the (σ_m-σ_a) plane can be obtained:

$$\sigma_a = \frac{\sigma_{a,1} - \sigma_{a,3}}{\sigma_{m,1} - \sigma_{m,3}} \sigma_m + \sigma_{a,1} - \frac{\sigma_{a,1} - \sigma_{a,3}}{\sigma_{m,1} - \sigma_{m,3}} \sigma_{m,1}, \tag{4}$$

and the line equation of the desired R_2 on the (σ_m-σ_a) plane is

$$\sigma_a = \frac{1 - R_2}{1 + R_2} \sigma_m. \tag{5}$$

Finally, the intersection point of the two lines corresponding to (4) and (5) will be solved. The abscissa value $\sigma_{m,2}$ of the intersection is presented as follows:

$$\sigma_{m,2} = -\frac{\sigma_{a,1}(\sigma_{m,1} - \sigma_{m,3}) - \sigma_{m,1}(\sigma_{a,1} - \sigma_{a,3})}{(\sigma_{a,1} - \sigma_{a,3}) - (\sigma_{m,1} - \sigma_{m,3})((1 - R_2)/(1 + R_2))}. \tag{6}$$

The model is derived based on a power S-N curve and can be used directly. If the model is applied based on an exponential S-N curve, the expression of $\sigma_{m,k}$ and $\sigma_{a,k}$ will be adjusted correspondingly according to the exponential S-N curve equation.

2.2.3. Piecewise Nonlinear CLD Model. The stress amplitude, mean stress, and stress ratio are the basic fatigue parameters required by the CLD formulation for a given cycle life [22]. The relationship between the three parameters is given as follows:

$$\sigma_a = \frac{1 - R}{1 + R} \sigma_m. \tag{7}$$

It can be seen from the above equation that any combination of two of these parameters can be used to describe the material behavior and establish a CLD model. For the fatigue life under different cycles loading, the relationship between the stress amplitude σ_a and stress ratio R is presented in Figure 2.

The desired S-N curves can be represented by the vertical lines through the corresponding R value and perpendicular to the x-axis, as can be seen from Figure 2. According to the variation characteristics of stress amplitude in the above line graph, the diagram can be divided into four different regions which, respectively, correspond to four loading conditions. Part I is under $-\infty \ll R \ll -1$ for compression-tension loading;

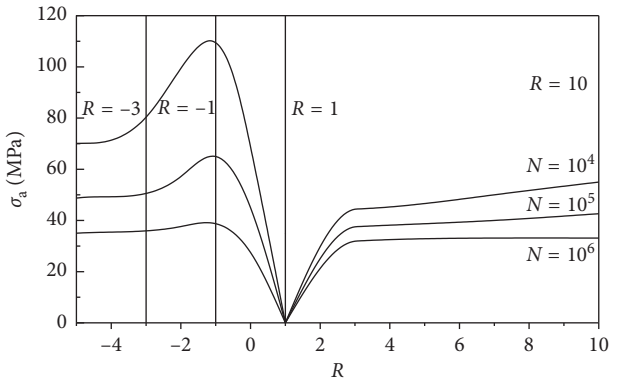

Figure 2: Representation of the PNL CLD model on the $R-\sigma_a$ plane.

Part II is under $-1 \ll R \ll 0$ for tension-compression loading; Part III is under $0 \ll R \ll 1$ for tension-tension loading; and Part IV is under $1 \ll R \ll \infty$ for compression-compression loading. The fatigue behavior of each part will be represented by the phenomenological equations, and the corresponding parameters in the model can also be obtained by applying the known data and appropriate boundary condition. For Parts I ($-\infty \ll R \ll -1$) and IV ($1 \ll R \ll \infty$), the stress amplitude is expressed as follows:

$$\sigma_a = (1-R)\left(\frac{A_{\text{I or IV}}}{R} + \frac{B_{\text{I or IV}}}{R^2}\right). \tag{8}$$

The A_I, A_{IV}, B_I, and B_{IV} in the above equation can be defined as follows:

$$\begin{aligned} A_{\text{I or IV}} &= -\sigma_a^{R=\pm\infty}, \\ B_I &= \frac{\sigma_a^{R=-1}}{2} - \sigma_a^{R=\pm\infty}, \\ B_{IV} &= \frac{\text{UCS}}{2} + \sigma_a^{R=\pm\infty}. \end{aligned} \tag{9}$$

If the S-N curve at $R = 10$ is available, it can be used to replace the S-N curve at $R = \pm\infty$. In addition, the boundary conditions of the above model will be modified accordingly. For Part II ($-1 \ll R \ll 0$) and Part III ($0 \ll R \ll 1$), the stress amplitude is expressed as follows:

$$\sigma_a = \frac{1-R}{A_{\text{II or III}} R^n + B_{\text{II or III}}}. \tag{10}$$

The exponent n is equal to 1 in Part II and is equal to 3 in Part III. When the S-N curve at $R = 0$ is taken into account, the A_{II}, A_{III}, B_{II}, and B_{III} in the above equation can be defined as follows:

$$\begin{aligned} A_{II} &= \frac{1}{\sigma_a^{R=0}} - \frac{2}{\sigma_a^{R=-1}}, \\ A_{III} &= \frac{2}{\text{UTS}} - \frac{1}{\sigma_a^{R=0}}, \\ B_{\text{II or III}} &= \frac{1}{\sigma_a^{R=0}}. \end{aligned} \tag{11}$$

Similarly, if the S-N curve at $R = 0.1$ is available, it can be used to replace the S-N curve at $R = 0$, and the boundary conditions of the above model will be adjusted accordingly. The model can be used directly based on a power S-N curve or an exponential S-N curve.

2.2.4. Bell CLD Model. The Bell CLD model derived by Harris obeys the following relationship [27–29]:

$$\frac{\sigma_a}{X} = f\left(1 - \frac{\sigma_m}{X}\right)^u \left(\frac{X'}{X} + \frac{\sigma_m}{X}\right)^v, \tag{12}$$

where X stands for the ultimate tensile strength and X' stands for the ultimate compression strength. The parameters f, u, and v are adjustable based on the function of fatigue life. A set of values for f, u, and v corresponding to different cycle stresses are different based on (12). This means a set of values for f, u, and v corresponding to different fatigue lives are also different. According to the fatigue data of the examined FRP material, these parameters are deduced to have a linear relationship with the logarithm of fatigue life:

$$\begin{aligned} f &= A_1 \log N + B_1, \\ u &= A_2 \log N + B_2, \\ v &= A_3 \log N + B_3, \end{aligned} \tag{13}$$

where A_i and B_i can be calculated by fitting (13) based on the available fatigue life data under different loading cycles. Here, each pair of f, u, and v values will be obtained by (12) to use nonlinear regression on the (σ_a-σ_m) plane. Different formulations of the parameter f have been built by Harris et al. based on the test data of different composite materials [27]. In the most recent study, the equation is as follows:

$$f = Ac^{-p}, \tag{14}$$

where both A and p are the functions of logarithmic life and c is defined as UCS/UTS. In order to obtain reasonable results, the values of $A = 0.71$ and $p = 1.05$ are often used for the given laminates. The model can be used directly based on a power S-N curve or an exponential S-N curve.

2.2.5. Boerstra CLD Model. An alternative formulation of the CLD developed by Boerstra can be used to predict fatigue life [30]. The mode can be applied when the given fatigue data are random data that are not necessarily required to belong to an S-N curve. The basic parameters required by the Boerstra model are the compression static strength data, tension static strength data, and fatigue life data under different cyclic stresses with constant amplitude. A modification based on the Gerber line is made by the model, and the shape of the diagram in the model is modified by introducing a variable exponent to replace the exponent 2. Different exponents are introduced under the tension or compression region. This obeys the following general relationship:

$$\text{For } S_m > 0,\ S_{ap} = S_{AP} * \left(1 - \left(\frac{S_m}{\text{UTS}}\right)^{\alpha T}\right), \tag{15}$$

$$\text{For } S_m < 0,\ S_{ap} = S_{AP} * \left(1 - \left(\frac{S_m}{\text{UCS}}\right)^{\alpha C}\right), \tag{16}$$

where the parameter S_{AP} is the peak amplitude of the constant life (CL) line for N_p cycles, the parameter S_{ap} is the stress amplitude for N_p and S_m, the parameter αT is the shape parameter of the CL line under the tension region, and the parameter αC is the shape parameter of the CL line under the compression region.

Based on the existing fatigue data of various laminate materials, the study shows that the slopes of the S-N lines under different mean stresses are variable. The S-N curve is steep under the tension region and has a smaller m value; the S-N curve is flatter under the compression region and has a higher m value. An exponential relationship between the curve slope m and the mean stress S_m is shown in the following equation:

$$m = m0 * e^{(-S_m/D)}, \tag{17}$$

$$\frac{S_1}{S_2} = \left(\frac{N_1}{N_2}\right)^{(1/m)}. \tag{18}$$

The parameter $m0$ is defined as the S-N curve slope on the log-log scale when $S_m = 0$, and the parameter D is the skewness parameter depended on m. The modeling process is as follows.

Firstly, an original model will be created by choosing the life value for N_p and assuming the initial values for $m0$, D, αT, and αC. Secondly, the value of S_{AP} will be solved as follows: (1) The expected value m corresponding to each S_m is calculated by (17), and each measured point data (S_m, S_a) are projected onto the N_p plane by (18). (2) Each mapping point S_{ap} is transposed onto the $S_m = 0$ axis by (15) or (16). (3) The S_{AP} in the model will be obtained by calculating the mean value of all individual points. Thirdly, the abovementioned parameters $m0$, D, αT, or αC will be optimized by obtaining the best fitting of the data points in the model. The least squares method will be adopted as the optimization method: (1) The logarithmic deviation of the fatigue life Δn is solved for each measured point: $\Delta n = \ln(N) - \ln(N_e)$, where $N_e = N_p (S_{ap,mod}/S_a)^m$ and N is the measured number of cycles. (2) The logarithmic deviation of the stress amplitude ΔS_a for each point is also solved: $\Delta S_a = \ln(S_{ap}) - \ln(S_{ap,mod})$, where $S_{ap,mod}$ is obtained by substituting the S_{AP} and the measured S_m into (15) or (16). Because both ΔS_a and Δn are obtained from logarithm form, they will be dimensionless. The shortest distance Δt between the S-N curve and each measured point data can be obtained, and the expression is as follows:

$$\Delta t = \text{sign}(\Delta S_a) * \sqrt{\left(\frac{1}{(1/\Delta S_a^2 + 1/\Delta n^2)}\right)}. \tag{19}$$

The standard deviation of all Δt is known as the total standard deviation SD_t. By optimizing the parameters $m0$, D, αT, or αC, the best fit can be achieved such that SD_t is minimal.

The model is derived based on a power S-N curve and can be used directly. If the model is applied based on an exponential S-N curve, (17) and (18) will be adjusted correspondingly according to the exponential S-N curve equation.

2.2.6. Kawai CLD Model. For the Kawai CLD, the model can be implemented by applying only one critical S-N curve, which is its basic characteristic [31, 32]. The critical S-N curve is defined as the experimentally determined S-N curve at R value, where R value is the ratio of USC to UTS for the examined material. The Kawai model can be realized by using the compression static strength data and tension static strength data as well as the critical S-N curve.

The mathematical formulation of the model will be represented in different forms based on the tensile region or the compressive region. The relationship is as follows:

$$\frac{\sigma_a^\gamma - \sigma_a}{\sigma_a^\gamma} = \begin{cases} \left(\frac{\sigma_m - \sigma_m^\gamma}{\text{UTS} - \sigma_m^\gamma}\right)^{2-\psi_x}, & \text{UTS} \gg \sigma_m \gg \sigma_m^\gamma, \\ \left(\frac{\sigma_m - \sigma_m^\gamma}{\text{UCS} - \sigma_m^\gamma}\right)^{2-\psi_x}, & \text{UCS} \gg \sigma_m \gg \sigma_m^\gamma, \end{cases} \tag{20}$$

where σ_m^γ and σ_a^γ are defined as the mean stress and stress amplitude for a given fatigue life N on the critical S-N curve and $\psi_x = \sigma_{\max}^\gamma/\sigma_B$, in which $\sigma_{\max}^\gamma$ is the maximum stress for a given fatigue life N on the critical S-N curve and σ_B (>0) is the static strength of the material $(\max\{||\text{UTS}||, ||\text{UCS}||\})$. The model can be used directly based on a power S-N curve or an exponential S-N curve.

The Kassapoglou model can be applied to obtain any desired S-N curve by using the sufficient compressive and tensile static strength data. However, the basic assumption of the model ignores the effects of different damage mechanisms. Due to lack of test data needed for the Kassapoglou model in this study, it is not described in detail here.

3. Test Setup

3.1. Specimen Forms and Material Properties. Fiber-reinforced 2060 Al-Li alloy laminates with the 2/1 structure and 3/2 structure were selected to carry out the loading test in this paper. The plate with center holes was adopted as the fatigue specimen. The form and the structure of the fatigue specimen are shown in Figures 3 and 4, respectively, and the property of the component material is shown in Table 1. The stress concentration factors which apply to net-section stress of the 2/1 laminates and 3/2 laminates are 2.57 and 2.56, respectively. The thickness of metal layers in the laminates is 1.9 mm, and the thickness of the fiber layer is 0.9 mm. The longitudinal direction of the metal material is used as the sampling direction of the metal layer in the laminates, and 0° is used as the laying direction of the fiber in the fiber layer. The UTS and UCS of the fiber-reinforced Al-Li alloy laminates with the 2/1 structure are 655 MPa and −521 MPa, respectively. The UTS and UCS of the fiber-reinforced Al-Li alloy laminates with the 3/2 structure are 665 MPa and −538 MPa, respectively.

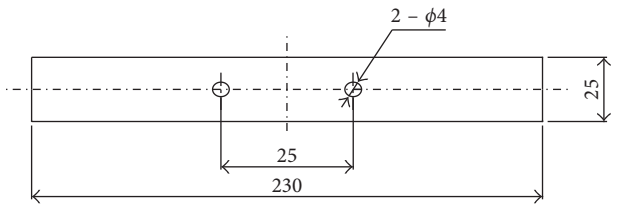

Figure 3: The fatigue S-N specimen of the laminate material (unit: mm).

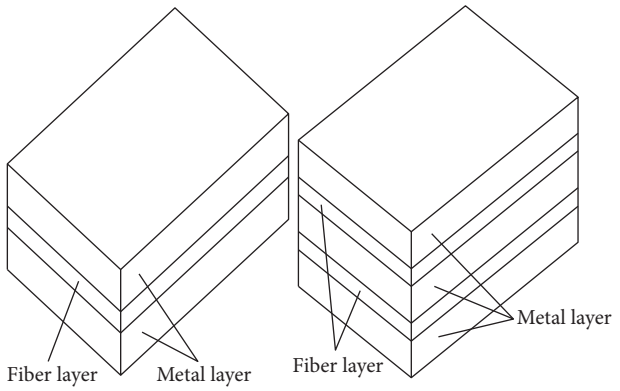

Figure 4: The structure diagram of 2/1 laminates and 3/2 laminates.

Table 1: Laminate component material property.

Material	Elastic modulus (GPa)	Poisson's ratio
Metal layer	72.4	0.3
Fiber layer	54.6	0.252

3.2. Test Equipment. The test equipment used in this test is a low-frequency fatigue testing machine, which is produced by Shimadzu Corporation. The model of the testing machine is EHF-EV101k1-040-1A, as shown in Figure 5. For the testing machine, the error value of the static load is less than ±0.5%, the dynamic load is less than ±3%, and the load range is ±100 kN.

3.3. Test Method. The test is carried out with reference to the National Aerospace Standard HB5287-96 [34]. The complete rupture of the metal layer in the laminates is treated as a fatigue failure criterion. The test is performed at room temperature in air environment, and the sine wave is used as the loading waveform. Three loading forms with different cycle characteristics were adopted in this study (constant amplitude loading with the stress ratio $R = 0.06$, that with the stress ratio $R = -1$, and Mini-Twist spectrum loading). The spectrum loading diagram is shown in Figure 6. Three stress levels are used in the S-N curve test, in which 3~5 samples are tested for each stress level, and the confidence level should be more than 95%.

3.4. Test Results. The test results obtained under different loading modes comprise six S-N curves, which are mainly in the range of $5 \times 10^4 \sim 5 \times 10^5$ cycles. In order to evaluate the fatigue lives by the phenomenological approach, it is important to select the appropriate expression of the S-N curve. The S-N curve equation can be expressed in different ways. In order to match the application of the CLD model, the fatigue data are fitted by using the standard HB5287-96 and are expressed by the power function that is now widely used. The linear relationship between the stress and the fatigue life is given by

$$\log N = a * \log\left\|\sigma_p\right\| + b. \tag{21}$$

The expression is derived from the classical power function formula of the S-N curve ($\sigma^a N = C$). After taking the logarithm on both sides of the formula, (21) is obtained, where the parameter a is the slope of the S-N curve and the parameter b is the intercept of the S-N curve. According to the theory of least squares regression, the test data can be fitted very well with the equation [24]. The values of σ_p for constant amplitude loading at $R = 0.06$ and $R = -1$ depend on $\max\{||\sigma_p||, ||\sigma_v||\}$, and the value of σ_p for Mini-Twist spectrum loading will depend on the baseline stress of the load spectrum. The S-N curves with the best fitting for each data set are presented in Figure 7, and the values of the parameters a and b are listed in Table 2.

Figure 5: Shimadzu electrohydraulic servocontrol fatigue test machine.

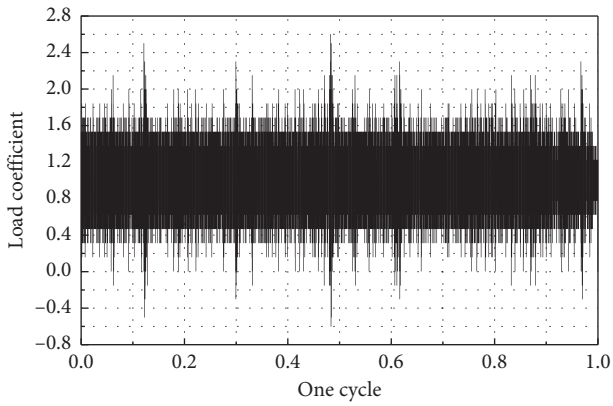

Figure 6: Mini-Twist loading diagram.

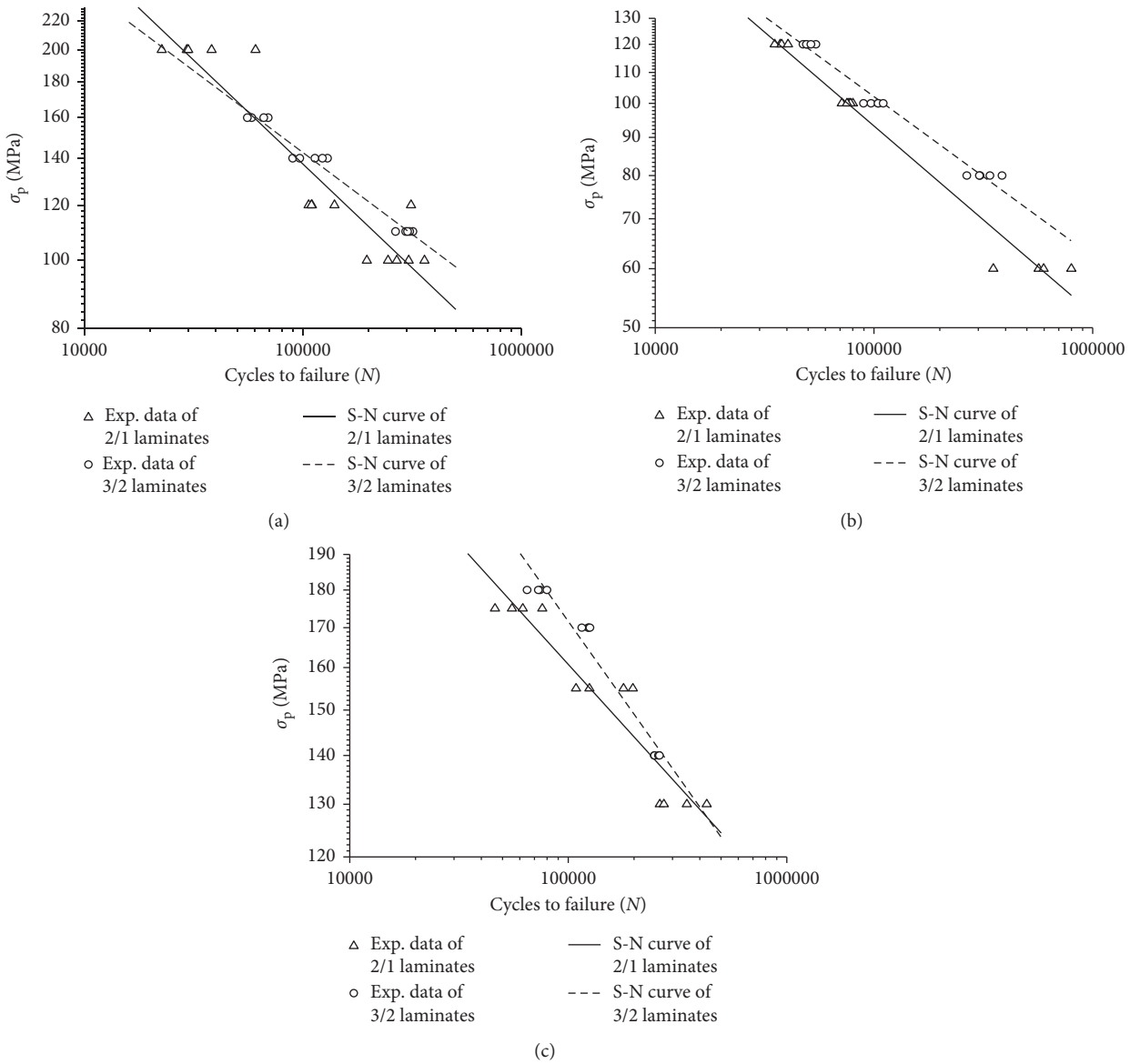

Figure 7: The S-N curve of 2/1 and 3/2 laminates: (a) $R = 0.06$; (b) $R = -1$; (c) Mini-Twist loading.

Table 2: Static strength data, fatigue test times, and S-N curve parameters for each laminate.

Material	UTS (Mpa)	UCS (Mpa)	Loading mode	Test times	a	b
2/1 laminates	655	−521.3	$R = 0.06$	15	−2.937	11.284
			$R = -1$	13	−3.883	12.648
			Mini-Twist	12	−5.626	17.428
3/2 laminates	665	−533.4	$R = 0.06$	14	−4.170	13.987
			$R = -1$	15	−4.570	14.182
			Mini-Twist	12	−4.666	15.432

4. Life Prediction under Spectrum Loading

4.1. Loading Cycle Counting. Many cycle-counting methods for variable amplitude fatigue loading have been used in the literature, which are from simple counting theory to complex algorithms. The simple theories include the peak, range-mean, and level crossing counting method, while the complex algorithms mainly refer to the rainflow counting and the related routine. In recent research, a discussion on the effect of the cycle-counting method was carried out by Passipoularidis in fatigue life prediction for composites. The research suggested that any cycle-counting methods would bring similar results [10].

Although the load spectrum will be unavoidably rearranged, even combined to produce full cycles, the rainflow-counting

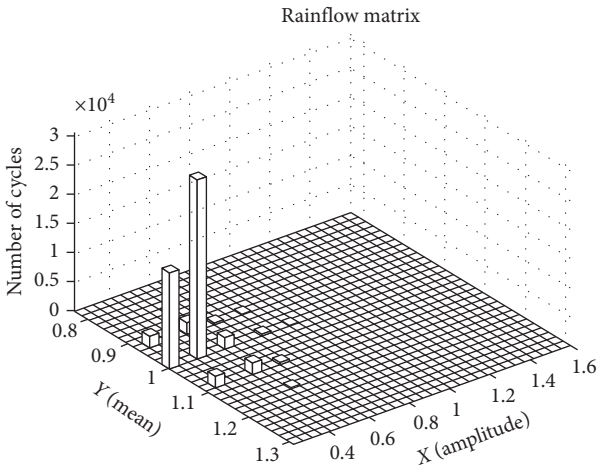

Figure 8: Diagram of statistical results for the rainflow-counting method.

method produces correct cycles with respect to the stress-strain relationship. Therefore, the rainflow method is adopted in this study as the counting method for the life prediction of fiber-reinforced Al-Li alloy laminates under Mini-Twist loading. The statistical result of the loop count of Mini-Twist loading is shown in Figure 8.

4.2. Constant Life Diagram Formulation. In this section, the allowable cycle number corresponding to R values that are not measured experimentally is evaluated. Through the above CLD model, fatigue life at R values that are not measured experimentally in spectrum loading is obtained. Because the power function is used as the expression of the S-N curve, the comparison of the models based on power curve function is introduced in detail, and the constant life diagram of two materials is presented in the following sections.

4.2.1. The 2/1 Laminates. As shown in Figure 9, three constant life curves corresponding to three life levels (37722, 76560, and 555904) are solved by each model for the 2/1 laminate material. The input data of the above CLD model mainly include the static strength data and the two available S-N curves at $R = -1$ and $R = 0.06$. The S-N curve at $R = -1$ and static strength data can be used to construct the formulas in the CLD models of Goodman and Kawai. For the Goodman model, the S-N curve at $R = -1$ can be used directly to construct the model. The ratio of UCS to UTS for the examined material is −0.795, which is the R value of the critical S-N curve in the Kawai CLD model. However, the S-N curve at this R value is not available. The critical curve in the model will be replaced by the closest curve in all curves at R values measured experimentally, that is, the curve at $R = -1$. Then, the critical curve is brought into the original model to solve the constant life curve.

The two existing S-N curves and static strength data are used for the construction of other models. For the piecewise linear CLD model, the linear interpolation method is directly used to obtain the constant life curve. For the piecewise nonlinear CLD model, because the S-N curve at $R = 0$ is not available, the S-N curve at $R = 0.06$ is used to replace the S-N curve at $R = 0$. The appropriate correction is made by solving the stress amplitude values corresponding to the three levels of life previously mentioned at $R = 0$. Then, the solved stress amplitudes, which are 95.985 MPa, 75.48 MPa, and 38.49 MPa, are brought into the model parameters to obtain three constant life curves. Due to the lack of a known condition under $-\infty < R < -1$ and $1 < R < \infty$ regions, and the information under $-\infty < R < -1$ and $1 < R < \infty$ regions is not required by Mini-Twist loading the model does not solve the constant life curve in the above area. For the Bell CLD model, since there are only two known R curves, (13) cannot be used directly to solve the value of f, u, and v. Firstly, the empirical value of f obtained by (14) is 0.903, and two given curves are substituted into (12) to obtain the value of u and v. Then, in order to obtain the linear relationship between u and logarithmic life, each u value is fitted linearly in the coordinate system where logarithmic life is used as the abscissa. Similarly, a linear relationship between v and logarithmic life can also be obtained. The obtained results are as follows: $u = 9.23 * \log(N) - 33.51$ and $v = 2.59 * \log(N) - 4.88$. Finally, to determine the constant life curve, the values of f, u, and v corresponding to the above logarithmic life are brought into the original model. In the Boerstra CLD model, the parameters m_0, D, and αT are optimized for different life data. For 37722 cycles, the values of m_0, D, and αT are 3.66, 114.09, and 0.779, respectively; for 76560 cycles, they are 3.70, 138.48, and 0.522, respectively; for 555904 cycles, they are 3.77, 204.09, and 0.354, respectively. Then, the optimized parameters are brought into the original model to obtain the constant life curve. Similar to the piecewise nonlinear CLD, this model does not calculate the constant life curve under $-\infty < R < -1$ and $1 < R < \infty$ regions.

In all the above methods, some models can construct the formulation by using only the $R = -1$ curve. Therefore, for the models constructed by using only the $R = -1$ curve, the S-N curve at $R = 0.06$ can be treated as the validated data. As shown in Figure 9, the prediction results of the Goodman and Kawai CLDs are not accurate enough for the 2/1 laminate material. For the Kawai model, the inaccurate results might be due to the difference between the used critical S-N curve and the one recommended by the Kawai model. In addition, the constant life curve under $-\infty < R < -1$ and $1 < R < \infty$ regions in the Bell model is obviously unreasonable, which may be due to the use of f empirical formula.

4.2.2. The 3/2 Laminates. As shown in Figure 10, three constant life curves corresponding to three life levels (47643, 110154, and 307610) are solved by each model for the 3/2 laminate material. The input data of the above CLD model mainly include the static strength data and the two available S-N curves at $R = -1$ and $R = 0.06$. Similar to 2/1 laminates, the S-N curve at $R = -1$ and static strength data can be used to construct the formulas in the CLD models of Goodman and Kawai. For the Goodman model, the S-N curve at $R = -1$

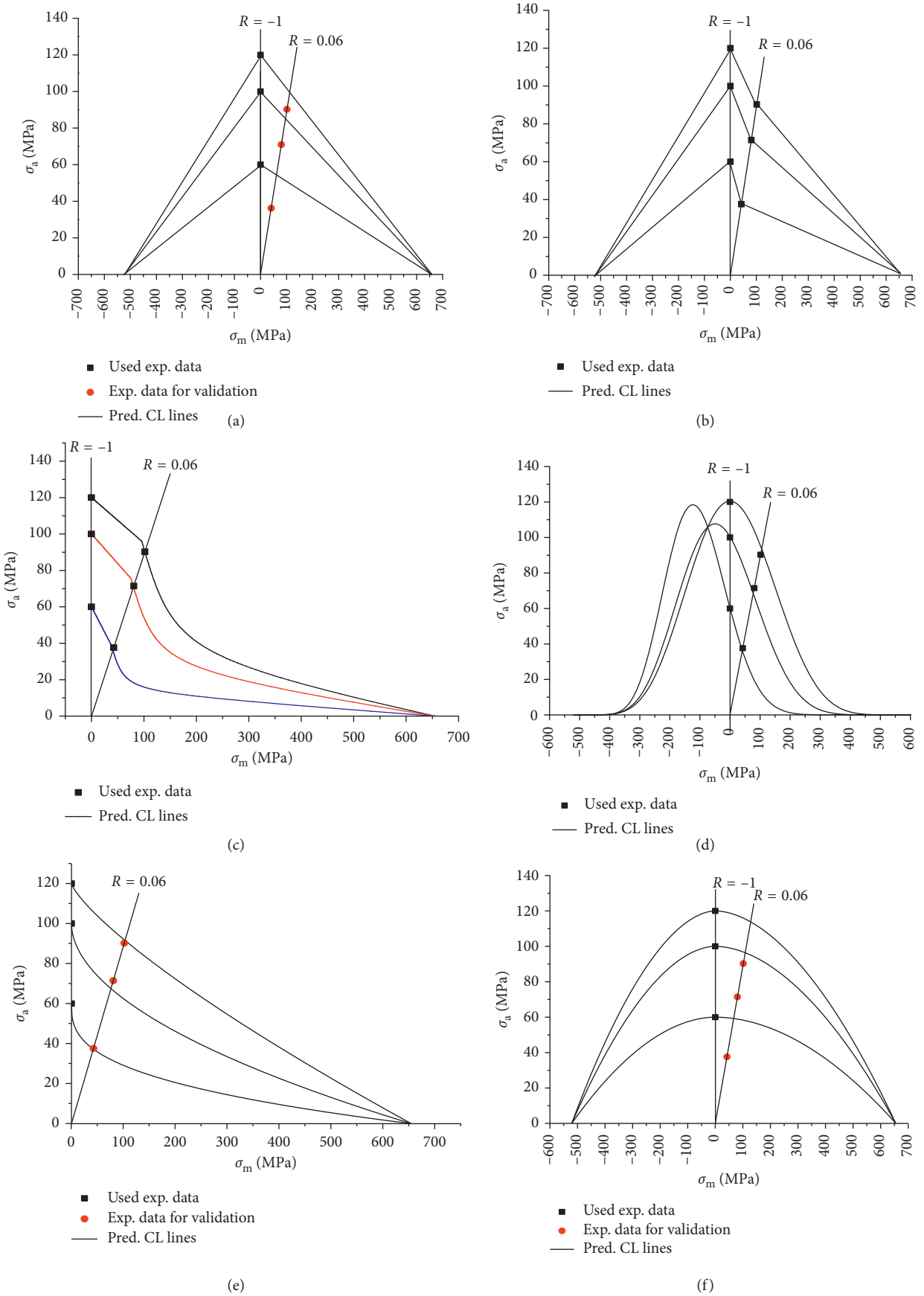

Figure 9: Constant life diagrams for $N = 37722$, 76560, and 555904 for 2/1 laminates: (a) Goodman; (b) piecewise linear; (c) piecewise nonlinear; (d) Bell; (e) Boerstra; (f) Kawai.

can be used directly to construct the model. The ratio of UCS to UTS for the examined material is −0.810, which is the R value of the critical S-N curve in the Kawai CLD model. Therefore, the S-N curve at $R = -1$ is used as the critical curve of 3/2 laminates. Finally, the critical curve is brought into the original model to solve the constant life curve.

The two existing S-N curves and static strength data are used for the construction of other models. For the piecewise linear CLD model, the linear interpolation method is directly used to obtain the constant life curve. For the piecewise nonlinear CLD, the model is accordingly modified, and the solved stress amplitudes values corresponding to the three levels of life at $R = 0$ are 85.49 MPa, 69.99 MPa, and 54.99 MPa, respectively. Then, the solved stress amplitudes are brought into the model parameters to obtain three constant life curves. Similar to 2/1 laminates, the constant life curve under $-\infty < R < -1$ and $1 < R < \infty$ regions is not solved for 3/2 laminates. In the Bell CLD, similar to 2/1 laminates, the empirical value of f obtained by (14) is 0.886, and the linear relationship between u and logarithmic life is obtained as follows: $u = 5.62 * \log(N) - 15.59$, and the linear relationship between v and logarithmic life is obtained as follows: $v = 2.37 * \log(N) - 3.53$. Finally, to determine the constant life curve, the values of f, u, and v corresponding to the above logarithmic life are brought into the original model. For the Boerstra CLD model, the parameters m_0, D, and αT are optimized for different life data. For 47643 cycles, the values of m_0, D, and αT are 4.570, 206.82, and 0.558, respectively; for 110154 cycles, they are 4.575, 242.10, and 0.482, respectively; for 307610 cycles, they are 4.579, 284.70, and 0.431, respectively. Then, the optimized parameters are brought into the original model to obtain the constant life curve. Similar to the piecewise nonlinear CLD, this model does not calculate the constant life curve under $-\infty < R < -1$ and $1 < R < \infty$ regions.

By comparing the S-N curve at $R = 0.06$, it is found that the prediction results of the Goodman and Kawai CLDs are also not reasonable for the examined material. For the Kawai model, the inaccurate results might also be due to the difference between the used critical S-N curve and the one recommended by the Kawai model. In addition, different from 2/1 laminates, the constant life curve obtained by the Bell CLD is reasonable under the whole region.

Thus, it can be seen that the prediction accuracy of all CLD models needs to be further verified in the following. In addition, if the S-N curve is expressed as an exponential function, then the allowable cycle number corresponding to R values that are not measured experimentally can also be evaluated by the above model.

4.3. Damage Accumulation. To predict fatigue life under variable amplitude stress history and further verify the accuracy of all models, the damage cumulative rule is introduced in this study. The prerequisites for the fatigue damage cumulative rule include the existence of equivalent fatigue damages at different cyclic stress levels and the existence of unique critical damage independent of the stress level.

The most widely used linear damage cumulative rule, that is, the Miner rule, states that the same cycle ratio n_i/N_i means the same fatigue damage, the cumulative fatigue damage produced by a variable amplitude load history containing n stress cycles equals to $\sum_{i=1}^{n} 1/N_i$ (N_i stands for the fatigue life under the ith stress cycle), and fatigue failure occurs when the cumulative fatigue damage reaches 1 (the critical damage value). This rule can be expressed as

$$\sum_{i=1}^{n} \frac{1}{N_i} = 1. \tag{22}$$

In order to predict the fatigue lives for two materials under spectrum loading, the linear damage criterion (PM) is used in the calculation of damage cumulative under Mini-Twist loading stress. In addition, the number of allowable cycles corresponding to loading stress can be solved by above models. Therefore, based on the rainflow-counting method and Miner damage criteria, the fatigue life of notched fiber-reinforced 2060 Al-Li alloy laminates under spectrum loading is predicted by applying different CLD models, and the prediction results are shown in Figure 11. It can be seen from Figure 11 that the difference in S-N curves obtained by different CLD models is very obvious. And the constant life curve obtained by the Bell CLD method for the 2/1 laminates is unreasonable, so the further verification is not made. Although the curvilinear trend of the CL line obtained by the BELL method for the 3/2 laminate is reasonable, the results of the S-N curve predicted by the model are also very inaccurate. This indicates that the method is not applicable for this type of material. The comparison results are shown and discussed in the next section.

5. Results and Discussion

A model error equation is used to describe the difference between the above predicted life and the mean life measured experimentally at the same stress level under spectrum loading in this paper [9]:

$$\text{Model error (Me)} = \log\left(\frac{N_{\text{model}}}{N_{\text{experiment}}}\right), \tag{23}$$

where N_{model} stands for the predicted life and $N_{\text{experiment}}$ stands for the mean life measured experimentally at the same stress level under the spectrum loading. The model error Me describes quantitatively how many orders of magnitude are different between the prediction results and the experimental results. A conservative error will be used as a negative Me, while a nonconservative error will be used as a positive Me.

Three levels of stress corresponding to the above life level are selected for each material, the stress levels for 2/1 laminates are 175 MPa, 155 MPa, and 130 MPa, respectively, and those for 3/2 laminates are 180 MPa, 170 MPa, and 140 MPa, respectively. Based on the mean life measured experimentally at three stress levels selected, (23) is used to calculate Me values generated by each model. The Me values generated by each model for different materials at three levels of stress

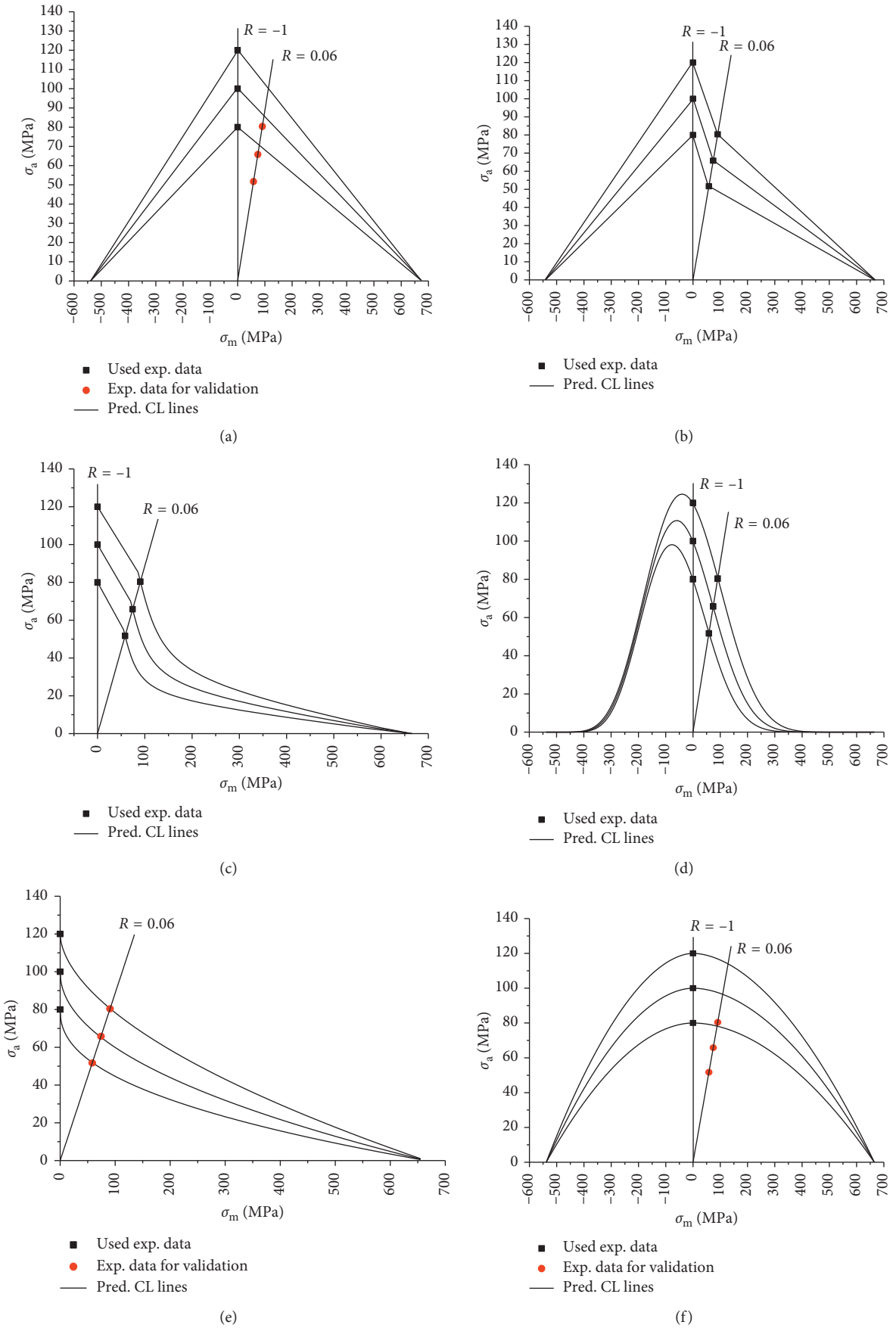

Figure 10: Constant life diagrams for N = 47643, 110154, and 307610 for 3/2 laminates: (a) Goodman; (b) piecewise linear; (c) piecewise nonlinear; (d) Bell; (e) Boerstra; (f) Kawai.

under spectrum loading are presented in Tables 3 and 4. According to the application of materials in engineering, it is believed that $-0.3 < \mathrm{Me} < 0.2$ indicates a good result.

The quantitative and qualitative comparison of each CLD model is carried out in this paper. To qualitatively analyze the prediction accuracy of model results, the S-N curves predicted by different models are compared with the experimental data under the Mini-Twist loading condition, which is shown in Figure 11. For these two materials, Goodman and Kawai CLD models overestimate the fatigue performance of the examined material, which leads to an optimistic assessment of fatigue life; the other models underestimate the fatigue behavior, which provides conservative prediction results. To further quantitatively validate the predicting ability of each model, the Me values are calculated by (23) and are shown in Tables 3 and 4. It can be seen that the lower Me values are provided by Goodman and Pwlinear models, which mean a good prediction result; the higher Me values are produced by other models, which mean an inaccurate prediction result.

The comparative analysis shows that, for the 2/1 laminates and 3/2 laminates, Goodman and Pwlinear CLD models can produce a reasonable and accurate result under Mini-Twist spectrum loading; the PNL, Boerstra, Bell, and Kawai models are considered to be not accurate enough for the life prediction under Mini-Twist spectrum loading. From the engineering point of view and on the safe side, the Goodman model is partial to optimistic, and the Pwlinear model is considered to be the most reliable. The Pwlinear model is not based on any assumption, and it is constructed by linear interpolation between fatigue data obtained by the experiment; therefore, the behavior of the examined material can be accurately described. Meanwhile, the Goodman model is constructed based on the experience assumption, which leads to an overly optimistic result. In four other models, apart from the PNL model, the Kawai, Bell, and Boerstra models are very sensitive to various factors. The accuracy of the Kawai model is influenced by the selected input data, the accuracy of the Bell model depends on the quality of the model parameter fitting, and the accuracy of the Boerstra model is determined by the optimization of the parameter estimation. Although the PNL model is derived without any assumption, it does not apply to describe the fatigue behavior of the examined material in this paper. In other words, the most fundamental factor influencing the prediction accuracy is the input data and basic assumptions for the model.

In terms of the experimental data needed to construct the model, it is obvious that Goodman and Kawai models are the least demanding model in all models, followed by Pwlinear and Bell models and finally Boerstra and PNL models. Of course, such a compromise may sacrifice the accuracy of their predictions for some models. In addition, the Pwlinear CLD model can also be constructed by using only one S-N curve at $R = -1$ so that the model is simplified into Goodman in this case. This will lead to a decline in the accuracy of the prediction. Meanwhile, Pwlinear and Boerstra models can also be constructed by using more S-N curves, which may provide more accurate results.

In terms of the assumption based on constructing the model, Pwlinear and PNL models are not based on any assumption, and other models are all based on certain assumptions. These assumptions stem from experience and experimental evidence, for example, the Goodman, BELL, Kawai, and Boerstra models. It is obvious that the model can be simplified by adopting the assumptions, and the fairly accurate results can be obtained under certain conditions. However, it is impossible to ensure that these models can be applied under different loading conditions, or for different materials.

6. Conclusions

The induction and comparison of recently developed and widely used CLD models for composite materials are implemented in this paper. For notched fiber-reinforced metal laminates under Mini-Twist spectrum loading, the effect of various constant life diagrams on the fatigue life prediction is studied and the prediction accuracy is quantified. The conclusions are summarized as follows:

(1) The CLD models developed for unnotched composites can be effectively applied to predict the fatigue life of notched fiber metal laminates under Mini-Twist loading. The selection of a suitable CLD model is crucial to the prediction accuracy of the total fatigue life for notched fiber-reinforced metal laminates under Mini-Twist spectrum loading. The effect of different models on the CLD shape is obvious. An inappropriate choice of the CLD model can lead to overly optimistic or conservative results, which will directly affect the fatigue performance assessment under Mini-Twist loading.

(2) Although some models such as Goodman and Kawai are developed for the purpose of minimizing the number of experimental data needed, this simplification undermines the accuracy to some extent in most cases. When there are more data available, these two models do not have the ability to use additional data. In other words, they cannot apply any other S-N curve to increase the prediction accuracy.

(3) The advantage of the Boerstra model is that the data do not need to be synthesized into the form of S-N curves and can be directly used. This means that the model can use directly the fatigue data under different cyclic stresses with constant amplitude to obtain the constant life curves. The accuracy of the Boerstra model is mainly determined by the optimization of the model parameters. Obviously, more fatigue life data under different cyclic stresses with constant amplitude are needed by the Boerstra model to improve the prediction accuracy.

(4) For the Bell model, the unified equation is used to depict the fatigue behavior under the tensile and compressive loading. The accuracy of the Bell model is reliable only when the model parameters can be

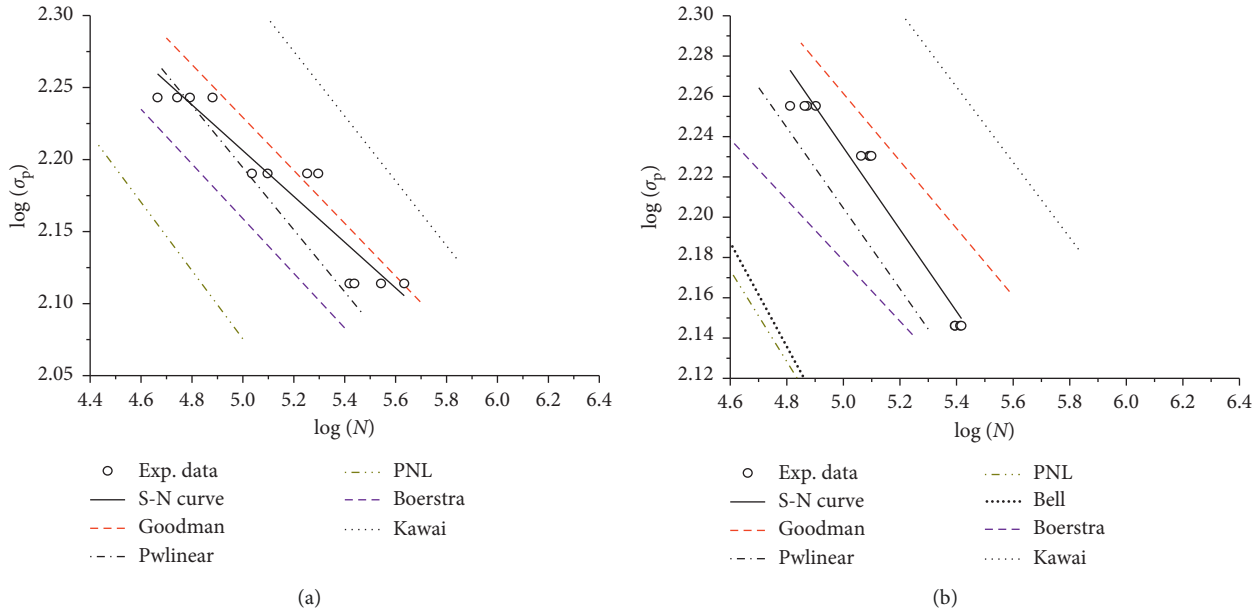

Figure 11: The life prediction results of each model: (a) 2/1 laminate; (b) 3/2 laminate.

Table 3: Comparison of model prediction results for the 2/1 laminates under spectrum loading.

Stress level (MPa)	175	155	130
Model	Me		
Goodman	0.134	0.065	0.098
Pwlinear	−0.010	−0.284	−0.226
PNL	−0.509	−0.607	−0.714
Boerstra	−0.360	−0.533	−0.428
Kawai	0.575	0.379	0.405

Table 4: Comparison of model prediction results for the 3/2 laminates under spectrum loading.

Stress level (MPa)	180	170	140
Model	Me		
Goodman	0.171	0.101	0.283
Pwlinear	−0.224	−0.300	−0.218
PNL	−0.713	−0.825	−0.772
Bell	−0.547	−0.680	−0.667
Boerstra	−0.508	−0.562	−0.324
Kawai	0.581	0.504	0.627

effectively fitted by using the fatigue life. But the method fitting the model parameters proposed by Harris does not always bring satisfactory results. At least, it does not apply to the above material.

(5) The PNL model is deduced by the relationship between the stress ratio and the stress amplitude and is expressed by the phenomenological equations. For the model parameter, it can be directly obtained by fitting to the available fatigue life data. The PNL model is not based on any assumptions, but it does not conform to the fatigue properties of the material studied in this paper.

(6) The Pwlinear model has been proved to have the best accuracy of all CLD models which are used to predict fatigue life of above laminates under the Mini-Twist loading. Although the model is relatively simple, it can provide more accurate results; if there are more S-N curves available, a more reasonable interpolation method between the available S-N curves will also improve the prediction accuracy.

Nomenclature

CLD: Constant life diagram
FRP: Fiber-reinforced polymer
UTS: Ultimate tensile strength
UCS: Ultimate compression strength
Exp. data: Experimental data
Pred. CL lines: Predicted constant lifelines
a: Slope of the S-N line on the log-log scale
b: Intercept of the S-N line on the log-log scale
N: Fatigue life
N_i: Allowable number of cycles under the ith stress cycle
Me: Model error
Pwlinear: Piecewise linear
PNL: Piecewise nonlinear
σ_a: Cyclic stress amplitude:
σ_m: Cyclic mean stress
σ_{eq}: Equivalent stress
R value: Stress ratio
S_a: Cyclic stress amplitude
S_m: Cyclic mean stress
S_{AP}: Peak amplitude of the CL line for N_p cycles
N_p: Reference number for the cycle life on the CL line

S_{ap}: Stress amplitude for N_p and S_m
αT: Shape parameters of the CL line under the tension region
αC: Shape parameters of the CL line under the compression region
D: Skewness parameter depended on m value
m: S-N line slope for σ_m
$m0$: S-N curve slope on the log-log scale when $S_m = 0$
N_e: Theoretical number of cycles on the Boerstra CLD model
Δn: Logarithmic deviation of the fatigue life
ΔS_a: Logarithmic deviation of the stress amplitude
Δt: Shortest distance between the S-N curve and each measured point data
SD_t: Total standard deviation
$S_{ap,mod}$: Modified stress amplitude by substituting S_{AP} and S_m into (15) or (16)
$S_{a,mod}$: Modified stress amplitude by calculating the average value of S_a
σ_m^γ: Mean stress for a given fatigue life N on the critical S-N curve
σ_{max}^γ: Maximum stress for a given fatigue life N on the critical S-N curve
σ_a^γ: Stress amplitude for a given fatigue life N on the critical S-N curve
σ_B: Tensile static strength of the material.

Conflicts of Interest

The authors declare that there are no conflicts of interest regarding the publication of this paper.

Acknowledgments

The authors gratefully acknowledge the financial support by the Natural Science Foundation of China (no. 51335003) and the Collaborative Innovation Center of Major Machine Manufacturing in Liaoning.

Supplementary Materials

Supplementary Figure 1: fatigue test specimen of 2/1 laminates. Supplementary Figure 2: testing process and failure mode for 2/1 laminates. Supplementary Figure 3: fatigue test specimen of 3/2 laminates. Supplementary Figure 4: testing process and failure mode for 3/2 laminates. Supplementary Table 1: fatigue test data of 2/1 laminates and 3/2 laminates at different stress levels under different loading modes. (*Supplementary Materials*)

References

[1] X. R. Wu and Y. J. Guo, "Development of methodology for predicting fatigue life of fiber reinforced metal laminates," *Advances in Mechanics*, vol. 29, no. 3, pp. 304–316, 1999, in Chinese.

[2] J. J. Homan, "Fatigue initiation in fiber metal laminates," *International Journal of Fatigue*, vol. 28, no. 4, pp. 366–374, 2006.

[3] P. Y. Chang, P. C. Yeh, and J. M. Yang, "Fatigue crack initiation in hybrid boron/glass/aluminum fiber metal laminates," *Materials Science and Engineering A*, vol. 496, no. 1-2, pp. 273–280, 2008.

[4] R. M. Frizzell, C. T. McCarthy, and M. A. McCarthy, "An experimental investigation into the progression of damage in pin-loaded fiber metal laminates," *Composites Part B: Engineering*, vol. 39, no. 6, pp. 907–925, 2008.

[5] J. W. Gummink, A. Vlot, T. J. De Vries, and W. van der Hoeven, "GLARE Technology Development 1997–2000," *Applied Composite Materials*, vol. 9, no. 4, pp. 201–219, 2002.

[6] C. A. J. R. Vermeeren, Th. Beumler, J. L. C. G. De kanter, O. C. van der Jagt, and B. C. L. Out, "GLARE design aspects and philosophies," *Applied Composite Materials*, vol. 10, no. 4-5, pp. 257–276, 2003.

[7] A. Hosoi, H. Kawada, and H. Yoshino, "Fatigue characteristics of quasi-isotropic CFRP laminates subjected to variable amplitude cyclic two-stage loading," *International Journal of Fatigue*, vol. 28, no. 10, pp. 1284–1289, 2006.

[8] W. X. Yao and N. Himmel, "A new cumulative fatigue damage model for fibre-reinforced plastics," *Composites Science and Technology*, vol. 60, no. 1, pp. 59–64, 2000.

[9] N. L. Post, S. W. Case, and J. J. Lesko, "Modeling the variable amplitude fatigue of composite materials: a review and evaluation of the state of the art for spectrum loading," *International Journal of Fatigue*, vol. 30, no. 12, pp. 2064–2086, 2008.

[10] V. A. Passipoularidis and T. P. Philippidis, "A study of factors affecting life prediction of composites under spectrum loading," *International Journal of Fatigue*, vol. 31, no. 3, pp. 408–417, 2009.

[11] M. M. Shokrieh and L. B. Lessard, "Progressive fatigue damage modeling of composite materials, part I: modeling," *Journal of Composite Materials*, vol. 34, no. 13, pp. 1056–1080, 2000.

[12] V. A. Passipoularidis, T. P. Philippidis, and P. Brondsted, "Fatigue life prediction in composites using progressive damage modeling under block and spectrum loading," *International Journal of Fatigue*, vol. 33, no. 2, pp. 132–144, 2011.

[13] J. W. Hu, M. Yu, and X. M. Wan, "Numerical simulation of fatigue failure for laminated composites," *Computer Simulation*, vol. 29, no. 4, pp. 64–67, 2012, in Chinese.

[14] S. U. Khan, R. C. Alderliesten, and R. Benedictus, "Delamination in fiber metal laminates (GLARE) during fatigue crack growth under variable amplitude loading," *International Journal of Fatigue*, vol. 33, no. 9, pp. 1292–1303, 2011.

[15] S. U. Khan, R. C. Alderliesten, and R. Benedictus, "Delamination growth in fibre metal laminates under variable amplitude loading," *Composites Science and Technology*, vol. 69, no. 15-16, pp. 2604–2615, 2009.

[16] S. U. Khan, R. C. Alderliesten, C. D. Rans, and R. Benedictus, "Application of a modified wheeler model to predict fatigue crack growth in fibre metal laminates under variable amplitude loading," *Engineering Fracture Mechanics*, vol. 77, no. 9, pp. 1400–1416, 2010.

[17] S. U. Khan, R. C. Alderliesten, and R. Benedictus, "Post-stretching induced stress redistribution in fibre metal laminates for increased fatigue crack growth resistance," *Composites Science and Technology*, vol. 69, no. 3-4, pp. 396–405, 2009.

[18] X. R. Wu and Y. J. Guo, "Fatigue life prediction of fiber reinforced metal laminates under variable amplitude loading," *Engineering Science*, vol. 1, no. 3, pp. 35–40, 1999, in Chinese.

[19] Y. Huang, J. Z. Liu, X. Huang et al., "Delamination and fatigue crack growth behavior in fiber metal laminates (Glare) under single overloads," *International Journal of Fatigue*, vol. 78, pp. 53–60, 2015.

[20] R. Talreja, "Fatigue of composite materials," in *Modern Trends in Composite Laminate Mechanics*, H. Altenbach and W. Becker, Eds., pp. 281–294, Springer-Verlag, Vienna, NY, USA, 2003.

[21] A. P. Vassilopoulos, B. D. Manshadi, and T. Keller, "Influence of the constant life diagram formulation on the fatigue life prediction of composite materials," *International Journal of Fatigue*, vol. 32, no. 4, pp. 659–669, 2010.

[22] A. P. Vassilopoulos, B. D. Manshadi, and T. Keller, "Piecewise non-linear constant life diagram formulation for FRP composite materials," *International Journal of Fatigue*, vol. 32, no. 10, pp. 1731–1738, 2010.

[23] J. F. Mandell, D. D. Samborsky, L. Wang, and N. K. Wahl, "New fatigue data for wind turbine blade materials," *Journal of Solar Energy Engineering*, vol. 125, no. 4, pp. 506–514, 2003.

[24] H. J. Sutherland and J. F. Mandell, "Optimized constant life diagram for the analysis of fiber glass composites used in wind turbine blades," *Journal of Solar Energy Engineering*, vol. 127, no. 4, pp. 563–569, 2005.

[25] T. P. Philippidis and A. P. Vassilopoulos, "Complex stress state effect on fatigue life of GRP laminates. Part I, experimental," *International Journal of Fatigue*, vol. 24, no. 8, pp. 813–823, 2002.

[26] T. P. Philippidis and A. P. Vassilopoulos, "Life prediction methodology for GFRP laminates under spectrum loading," *Composites Part A: Applied Science and Manufacturing*, vol. 35, no. 6, pp. 657–566, 2004.

[27] B. Harris, "A parametric constant-life model for prediction of the fatigue lives of fiber-reinforced plastics," in *Fatigue in Composites*, B. Harris, Ed., pp. 546–568, Woodhead Publishing Limited, Cambridge, UK, 2003.

[28] N. Gathercole, H. Reiter, T. Adam, and B. Harris, "Life prediction for fatigue of T800/5245 carbon-fiber composites: I. Constant-amplitude loading," *International Journal of Fatigue*, vol. 16, no. 8, pp. 523–532, 1994.

[29] M. H. Beheshty and B. Harris, "A constant life model of fatigue behavior for carbon fiber composites: the effect of impact damage," *Composites Science and Technology*, vol. 58, no. 1, pp. 9–18, 1998.

[30] G. K. Boerstra, "The multislope model: a new description for the fatigue strength of glass reinforced plastic," *International Journal of Fatigue*, vol. 29, no. 8, pp. 1571–1576, 2007.

[31] M. Kawai and M. Koizumi, "Nonlinear constant fatigue life diagrams for carbon/epoxy laminates at room temperature," *Composites Part A: Applied Science and Manufacturing*, vol. 38, no. 11, pp. 2342–2353, 2007.

[32] M. Kawai, "A method for identifying asymmetric dissimilar constant fatigue life diagrams for CFRP laminates," *Key Engineering Materials*, vol. 334-335, pp. 61–64, 2007.

[33] C. Kassapoglou, "Fatigue life prediction of composite structures under constant amplitude loading," *Journal of Composite Materials*, vol. 41, no. 22, pp. 2737–2754, 2007.

[34] HB5287-1996, *Test Method for Axial Loading Fatigue of Metallic Materials*, Aviation Industry Corporation of China, Beijing, China, 1996.

[35] P. Johannesson, T. Svensson, and J. deMaré, "Fatigue life prediction based on variable amplitude tests-methodology," *International Journal of Fatigue*, vol. 27, no. 8, pp. 954–965, 2005.